Effects of Plume Impingement on a Momentum Bias Communications Satellite

S.M. Fox*
RCA Corporation, Princeton, New Jersey

The Satcom communications satellite is structured such that the solar array panels are affected by significant impingement due to the inclination control jets. Theoretical predictions of the plume induced disturbance torques and forces were estimated via computer modeling. These predictions were doubled for use as the design criteria for the attitude control subsystem and for the allocation of fuel. Once the satellite was in geosynchronous orbit, several tests were performed to check and validate both the attitude control design and the plume modeling. The results of these tests indicated that the actual plume disturbances were approximately equal to the design criteria values (double the theoretically predicted values) and within the limits of the control system. In addition, it was indicated that the solar array surface properties/geometry modeling is critical in precise predictions of plume impingement effects.

Nomenclature

A = constant used in the plume density curve fit equation
C_p = constant pressure specific heat
C_v = constant volume specific heat
F = force vector
$F_n(F_t)$ = normal (tangential) force per unit area acting on the surface in the plume flowfield
H = satellite bias momentum level
L = characteristic length of the surface in the plume flowfield
M = torque vector
M = Mach number
M_e = Mach number at the jet nozzle exit plane
$\dot{m}$ = total mass flow rate through the jet
$p_i(q_i)$ = normal (tangential) momentum component of the incident plume flow
$p_r(q_r)$ = normal (tangential) momentum/component of the reflected plume flow
$p\omega(q\omega)$ = normal (tangential) component of the re-emitted plume flow molecules with a Maxwellian distribution at the surface temperature, T_ω
R = position vector
R = specific gas constant (ideal gas constant divided by the molecular weight of the specific gas under consideration)
r = radial distance from the jet to the point of interest on the surface in the flowfield
r_e = jet nozzle exit radius
S = molecular speed ratio
T_0 = stagnation temperature of the gas
T_L = local temperature in the plume flowfield
T_ω = temperature of the surface in the plume flowfield
t = plume calibration test pulse width
U = plume flow velocity
U_l = limiting velocity of the plume flow
x,y,z = Cartesian components of the radial distance r from the jet to the point of interest on the surface in the plume flowfield
α = relative solar array position
β_0 = ratio of thermal velocity to free stream velocity U_l for the reflected plume flow
γ = specific heat ratio
$\Delta\phi$ = satellite roll error change
θ = angle of incidence of the plume flow on the surface of interest
θ_∞ = limiting turning angle for inviscid flow at the jet nozzle exit Mach number
θ_e = cone half angle of the jet nozzle
$\bar{\lambda}$ = mean free path of the gas molecules
ρ = plume flowfield density
$\sigma_n(\sigma_t)$ = normal (tangential) accommodation coefficient
τ_c = satellite control torque
τ_d = satellite disturbance torque
τ_x = satellite net yaw torque
τ_{xB} = component of satellite yaw torque due to geometrical location of jet with respect to the satellite center of mass
τ_{xp} = component of satellite yaw torque induced by plume impingement
ν = Prandt-Meyer turning angle
Ω_{eff} = source flow solid angle

Presented as Paper 81-1383 at the AIAA/SAE/ASME 17th Joint Propulsion Conference, Colorado Springs, Colo., July 27-29, 1981; submitted Aug. 8, 1981; revision received May 19, 1982.

*Principal Member of the Technical Staff, Guidance & Control Group, Attitude Control Systems. AIAA Member.

Introduction

PRESENT and future satellites which require jets for orbit adjustment and/or attitude control have satellite surfaces, antennas, solar panels, and other satellite components located within the exhaust plume of the jets. Plume impingement on any of these surfaces will cause disturbance torques which must be absorbed and/or controlled by the satellite attitude control system. Similarly, during any orbit-adjust maneuver, plume impingement on any satellite surfaces or components will introduce an inefficiency due to drag which must be included as an additional fuel requirement for the expected satellite mission life. Demands of the present day design of satellites, such as communications satellites which specify overall pointing accuracies of 0.1 deg or better and operational mission life expectancies of 8 years or more, necessitate reliable predictions of these plume impingement disturbances.

To approximate the flowfield due to jet exhaust plume impingement, methods have been developed which incorporate both the characteristics of the exhaust gas (stagnation temperature, stagnation pressure, chemical composition, ratio of specific heats) and the characteristics of the nozzle (expansion ratio, throat diameter, cone half angle). Having defined the plume flowfield, the disturbance torques

and forces can be calculated and incorporated into the final design considerations and requirements of the satellite. A specific plume model and its application to the Satcom I communications satellite is discussed.

Satellite Attitude Control

The first in a series of such satellites, shown in Fig. 1, was launched and inserted into a geosynchronous orbit in December, 1975. The satellite is three-axis stabilized with a momentum bias control system. Normal environmental disturbances (gravity gradient, magnetic residuals, solar pressure) are controlled by a closed-loop system employing magnetic torquers along the roll (Y) and the yaw (X) axes[1] and by a momentum storage wheel along the pitch (Z) axis.[2] During a stationkeeping maneuver, jets are used to move the satellite in the north/south or the east/west direction and to maintain the attitude control of the satellite.

As shown in Fig. 1, during an inclination-adjust maneuver (north/south stationkeeping), jets 1-4 are used to obtain the required orbit correction. These same jets are off-pulse modulated to control the satellite attitude.[3] The satellite solar array and support boom are directly in the exhaust plume flowfield of jets 1-4. In order to determine the stability of the satellite with the proposed control system, a calculation of the disturbances due to plume impingement is required. The control torques must be sufficient to compensate for the expected disturbances with adequate margin. Also, in order to provide a sufficient fuel budget for the planned mission life of the satellite, a calculation of the drag force (loss) on the solar array due to plume impingement must be made.

Plume Flowfield Approximation

A plume flowfield analysis of the monopropellant hydrazine (N_2H_4) decomposition motor used on the satellite had previously been performed using a method of characteristics (MOC) approach.[4] Strictly speaking, the method of characteristics is a numerical procedure that "marches" systematically through the flowfield calculating the flow characteristics (velocity, density, Mach number, etc.). The method assumes that small disturbances in a two-dimensional, supersonic flow are propagated in the form of pressure waves along the Mach lines, that these lines are also lines of constant perturbation potential, and that the vector change in velocity produced by a pressure wave must accordingly have a direction normal to the Mach direction.[5] Since information does not propagate upstream in a supersonic flowfield, the flow characteristics preceding a Mach line are uniquely determined. The transition parameters across the Mach line are then approximated and the flow characteristics following the Mach line are integrated to provide a smooth transition. This procedure is repeated for the next Mach line and the flow characteristics are systematically calculated by marching in this manner throughout the flowfield. Constant property contours obtained by the MOC approach are depicted in Fig. 2.

One of the constant properties associated with the contours of Fig. 2 is the plume flowfield density. These constant density profiles can be approximated by a curve fit which is a function of r, the radial distance from the jet to the point of interest on the surface in the flowfield, and a function of θ, the angle of incidence of the plume flow on the surface (see Fig. 3). An approximate curve fit to the MOC density contours in the region of the solar array is of the form

$$\rho = (\dot{m}/U_j\Omega_{\text{eff}})(\cos^8\theta + A\cos^4\theta)/r^2 \qquad (1)$$

where $\dot{m}$ is the total mass flow of the jet and A a constant equal to 0.06. For this approximation, the jet is assumed to be a source flow of solid angle, Ω_{eff}, defined by the relation

$$\Omega_{\text{eff}} = 2\pi\int_0^{\theta_\infty}(\cos^8\theta + A\cos^4\theta)\sin\theta\,d\theta \qquad (2)$$

where θ_∞ is the limiting turning angle for inviscid flow at the nozzle exit Mach number (see Fig. 4) and is defined as

$$\theta_\infty = \nu(M=\infty) - \nu(M=M_e) + \theta_e \qquad (3)$$

Here, ν is the Prandt-Meyer turning angle for Mach number M, M_e is the Mach number at the nozzle exit plane, and θ_e is the cone half angle of the nozzle.

Since the region of interest (the solar array) is near the centerline of the plume flow and far from the jet nozzles

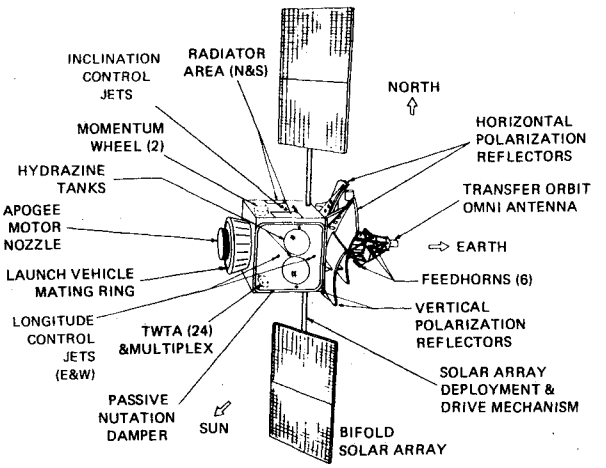

Fig. 1 Satellite configuration.

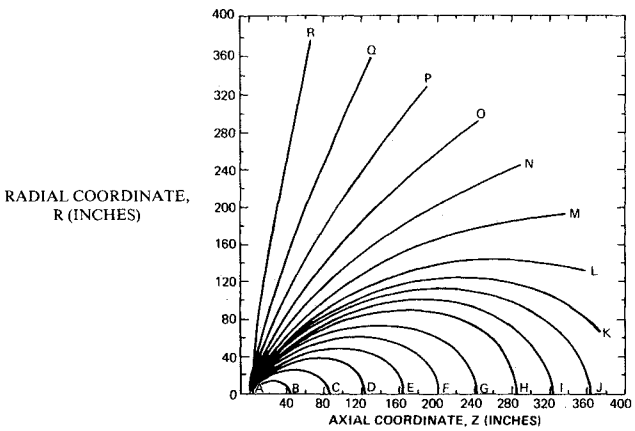

Fig. 2 Far field plume constant property contours.

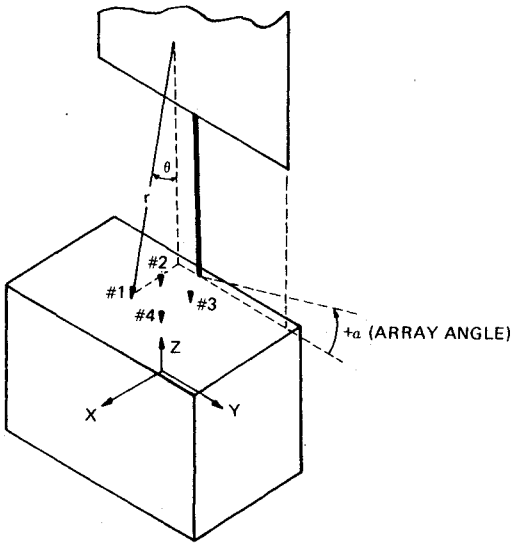

Fig. 3 Plume flow/satellite geometry.

(distances large compared to the nozzle exit diameter), the velocity of the plume flow can be assumed to have reached the limiting value U_l, defined by

$$U_l = \sqrt{2\gamma RT_0/(\gamma - 1)} \tag{4}$$

In this expression, γ is the specific heat ratio (C_p/C_v), R is the specific gas constant (the ideal-gas constant divided by the molecular weight of the specific gas under consideration), and T_0 is the stagnation temperature of the gas (dissociated hydrazine). The appropriate jet nozzle parameters and gas characteristics required in Eqs. (1-4) and the resulting calculated exhaust plume parameters are listed in Table 1.

A comparison of the MOC density contours with those generated through Eq. (1) in the region of the solar array is shown in Fig. 5. No appreciable difference can be observed between the shapes of the curves in Fig. 5, but the density calculated by the curve fit approximation is 1.59×10^{-14} slugs/in.^{3} compared to 1.45×10^{-14} slugs/in.^{3} predicted by the MOC approach. This 10% difference is small compared to other uncertainties in the plume disturbance calculations and will provide a more conservative estimate.

Force and Moment Calculations

In order to calculate the plume impingement forces and subsequent induced disturbance torques about the satellite center of mass, free molecular flow rather than continuum flow gas dynamics is assumed. The basic criteria used in determining the appropriate gas dynamics is the ratio $\bar{\lambda}/L$, where $\bar{\lambda}$ is the mean free path of the gas molecules and L a characteristic length of the surface in the flowfield. The requirement used in this analysis for continuum flow theory is that $\bar{\lambda}/L$ approaches infinity in the region of interest. The satellite configuration depicted in Fig. 1 and the associated jet exhaust gas parameters provide $\bar{\lambda}/L$ values for which the free molecular flow theory is appropriate.

On the basis of free molecular theory,[6] the normal force F_n and the tangential force F_t per unit area acting on the surface in the plume flowfield are

$$F_n = (\rho U^2/2S^2)\Big(\{[(2-\sigma_n)S\sin\theta/\sqrt{\pi}] + (\sigma_n/2)\sqrt{T_\omega T_L}\}e^{-(S\sin\theta)^2} + \{(2-\sigma_n)[(S\sin\theta)^2 + \tfrac{1}{2}] + (\sigma_n/2)\sqrt{\pi T_\omega/T_L}S\sin\theta\}[1+\operatorname{erf}(S\sin\theta)]\Big) \tag{5}$$

and

$$F_t = (\sigma_t \rho U^2 \cos\theta/2S\sqrt{\pi})\{e^{-(S\sin\theta)^2} + \sqrt{\pi}S\sin\theta[1+\operatorname{erf}(S\sin\theta)]\} \tag{6}$$

assuming a coordinate system shown in Fig. 6. In Eqs. (5) and (6), ρ is the plume density as defined by Eq. (1), U is the plume velocity as defined by Eq. (4), T_ω is the temperature of the surface of the flowfield, and S is defined as

$$S = U_l/\sqrt{2RT_L} = \sqrt{2\gamma RT_0/(\gamma-1)}/\sqrt{2RT_L} = \sqrt{[\gamma/(\gamma-1)](T_0/T_L)} \tag{7}$$

(T_L is the local temperature in the plume flowfield.) Now, σ_n and σ_t are the conventionally defined normal and tangential accommodation coefficients, respectively,

$$\sigma_n = (p_i - p_r)/(p_i - p_\omega) \tag{8}$$

$$\sigma_t = (q_i - q_r)/(q_i - q_\omega) \tag{9}$$

where p and q are the normal and the tangential momentum components, respectively. The subscripts i and r refer to the incident and reflected flux while p_ω and q_ω denote, respectively, the normal and tangential momentum components of the molecules which are re-emitted with a Maxwellian distribution at the surface temperature T_ω. (Obviously, q_ω must be zero.[6])

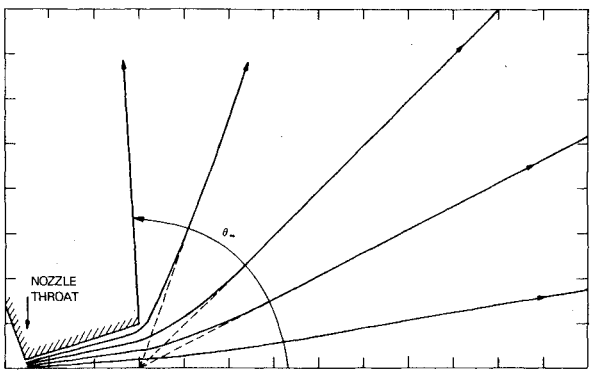

Fig. 4 Development of radial far field plume flow from an inviscid nozzle.

Table 1 Nozzle parameters and gas characteristics of an N_2H_4 jet

Parameter	Value
$\dot{m}$	1.85×10^{-5} slugs/s
U_l	1.0062×10^{-5} in./s
Ω_{eff}	44.32 deg
Θ_∞	89.85 deg
M_e	5.32
θ_e	15 deg
γ	1.26
R	18,540 lbf-in./°R·lbm·mole
T_0	2000°R
r_e	0.1 in.

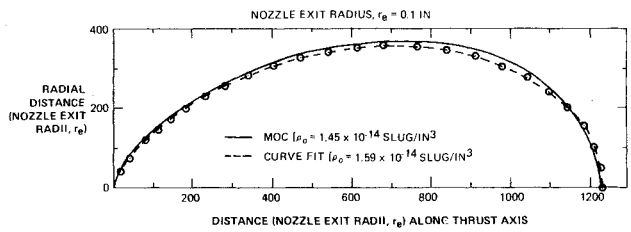

Fig. 5 Typical constant density contour comparison.

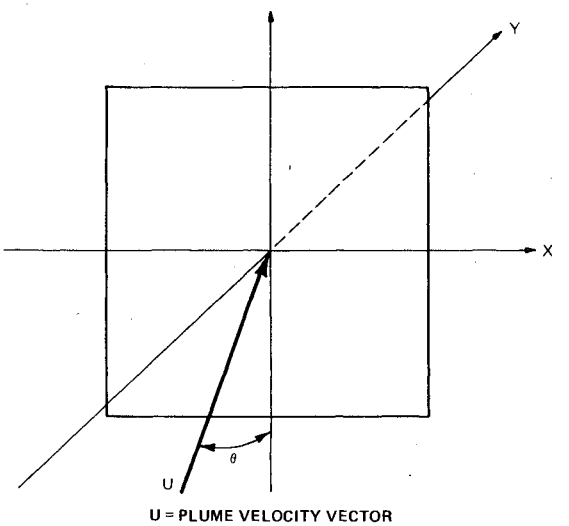

Fig. 6 Coordinate system for free molecular flow force equations.

The accommodation coefficients must be determined prior to the force calculations and this requires a knowledge of the characteristics of the gas/surface collision interaction. For the hypothetical cases of 1) entirely specular reflection, one would have $\sigma_n = \sigma_t = 0$; while 2) for an entire diffuse reflection, which has been completely accommodated to the surface temperature T_ω, one would have $\sigma_n = \sigma_t = 1$. In general, it is to be expected that these two parameters will be independent. Since the exact values of σ_n and σ_t are not known for most cases, a worst case assumption of $\sigma_n = \sigma_t = 1$ is used to determine the maximum disturbances that can be expected.

For very high velocities and thus very high values of S, the limiting forms of Eqs. (5) and (6) are

$$F_n = \rho U^2 [(2-\sigma_n)\sin^2\theta + \sigma_n \beta_0 \sin\theta] \tag{10}$$

$$F_t = \rho U^2 \sigma_t \cos\theta \sin\theta \tag{11}$$

where

$$\beta_0 = \sqrt{\pi (T_\omega / T_0)(\gamma - 1)/4\gamma} \tag{12}$$

Using the plume/satellite coordinate system shown in Fig. 3, the above force equations become

$$F_x = \rho U^2 \sigma_t yx/r^2 \tag{13}$$

$$F_y = \rho U^2 [(2-\sigma_n)y^2 + \sigma_n \beta_0 yr]/r^2 \tag{14}$$

$$F_z = \rho U^2 \sigma_t yz/r^2 \tag{15}$$

Similarly, the torques per unit area of the impingement surface are obtained through the relationship

$$M = R \times F \tag{16}$$

The total forces and torques due to plume impingement affecting the satellite are calculated by integrating Eqs. (13-16) over the entire area of the surface in the plume flowfield.

Predicted Plume Impingement Disturbances vs Satellite Attitude Control Design

Using this technique for estimating the disturbances due to plume impingement, the satellite control system during north/south stationkeeping (orbit inclination adjust) was analyzed. It should be emphasized that for the attitude control design, the nominal plume disturbance torques predicted by this mathematical model were doubled in order to compensate for all the uncertainties associated with the model. These doubled nominal values are shown as the plume disturbances (torques and forces) in Figs. 7-12.

The available control torques about the yaw (X) axis and roll (Y) axis of the satellite are each nominally 0.488 in.-lb per thruster (assuming an initial thrust level of 0.122 lbf). In order to maintain a minimum control margin of 25% (ratio of control torque to disturbance torque (τ_c/τ_d) greater than 1.25/1.00), the array is limited to positions with a predicted plume disturbance torque of 0.390 in.-lb (design limit) or less. From Figs. 7 and 8, it can be seen that the required minimum 25% control margin is achieved for array positions approximately between 86 and 94 deg. Thus, with this satellite configuration, the north/south stationkeeping maneuver must be accomplished with the solar array positioned within ±4 deg of the null position. (The null position is defined as that which aligns the solar array to symmetrically bisect the combined plume of the four thrusters.)

The disturbance forces (twice the predicted value) due to plume impingement on the solar array are shown in Figs. 10-12. For a worst case positioning of the solar array, the maximum expected efficiency loss due to plume drag (Z-plume force/thrust) is approximately 5%. The overall satellite fuel budget for the expected mission life was appropriately modified to account for this additional inefficiency.

Solar Array Position/Plume Impingement Calibration

Once the satellite was in the drift orbit (post-AKM burn) and had achieved Earth lock, it was necessary to perform a series of calibration tests in order to determine the solar array position sensitivity with respect to the jet plume-induced disturbances, i.e., determine the array position associated with minimum plume impingement disturbances. These calibration tests also afforded the opportunity to compare the actual plume disturbances to those predicted by the model.

The basic calibration test consisted of a 6 s pulse from a particular combination of jets while observing the relative change in the measured satellite roll error. Both the initiation and termination of the pulse were commanded via the ground control computer, thus assuring a high degree of accuracy in the actual duration of the pulse. In addition, the satellite bias momentum level was noted both before and after the pulse and the pressure associated with the fuel system was recorded in order to estimate the current thrust level of the jets. These calibration tests were performed several times at various solar

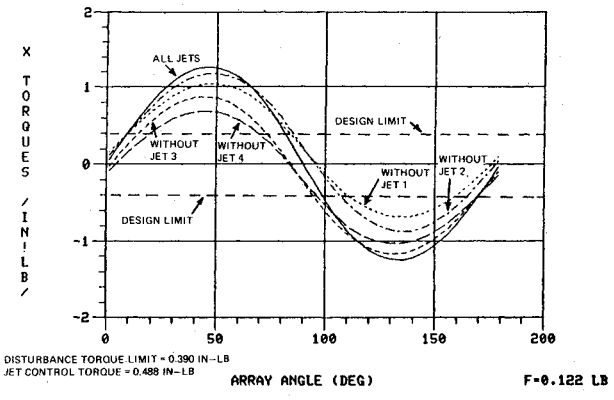

Fig. 7 Design criteria X plume impingement torques.

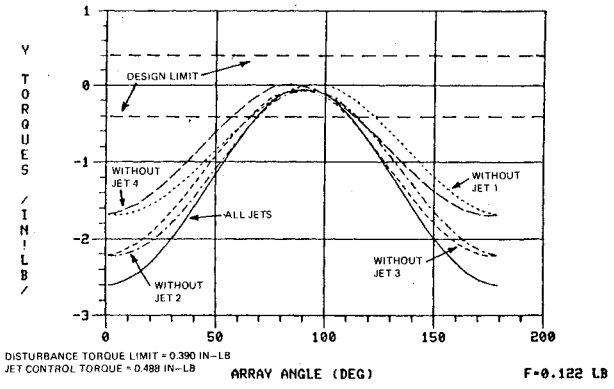

Fig. 8 Design criteria Y plume impingement torques.

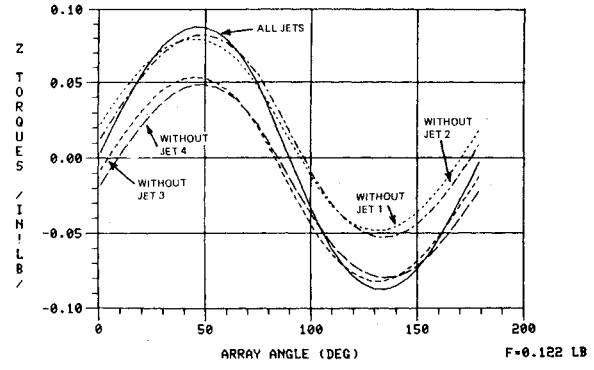

Fig. 9 Design criteria Z plume impingement torques.

array positions at selected times in the satellite orbit in order to assure a range of satellite/solar array/sun geometries.

Each calibration test provided the following data: relative roll error change ($\Delta\phi$) observed via an Earth sensor assembly (ESA) consisting of two scanning bolometers, satellite bias momentum level H, and the duration t of the pulse from the appropriate jet combination. These data allow the calculation of the net yaw torque (τ_x) affecting the satellite motion via the equation

$$\tau_x = (H/t)\tan(\Delta\phi) \tag{17}$$

A significant number of calibration tests were performed and the useful data are listed in Table 2. Having completed the tests and having reduced the data, the satellite ground control personnel were able to orient the solar array and optimize the inclination-adjust maneuvers.

Disturbance Torques Due to Plume impingement

Having obtained the above described calibration test data, it is possible to estimate the magnitude of the plume induced yaw torque and to compare this measured value to that predicted. The net yaw torque (τ_x) from any combination of jets 1-4 has two components: one (τ_{xp}) associated with the plume of the relevant jets and the other (τ_{xB}) provided by the physical location of the jets with respect to the satellite center of mass (CM), i.e., $\tau_x = \tau_{xp} + \tau_{xB}$. (It should be noted that the net roll and pitch torques also have two components.) Equation (17) thus provides a means of estimating the plume torque

$$\tau_{xp} = (H/t)\tan(\Delta\phi) - \tau_{xB} \tag{18}$$

The magnitude of τ_{xB} can be calculated in a straightforward manner by using the measured physical location and angular orientation of each jet and the current thrust level which is determined via telemetry from the satellite. It should be noted that for this analysis, all uncertainties associated with τ_{xB} due to CM location, jet location orientation, and thrust level are included as part of τ_{xp}.

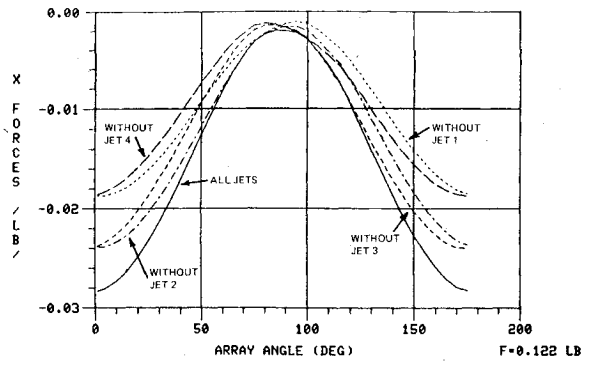

Fig. 10 Design criteria X plume impingement forces.

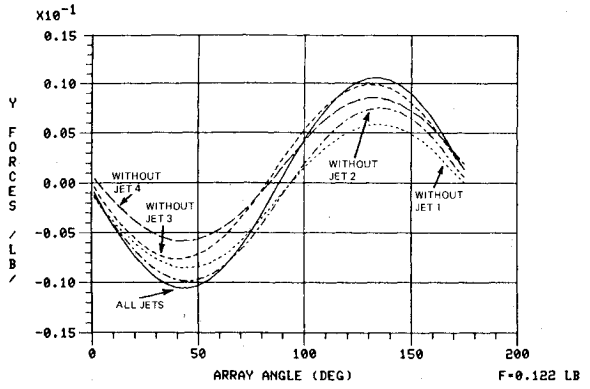

Fig. 11 Design criteria Y plume impingement forces.

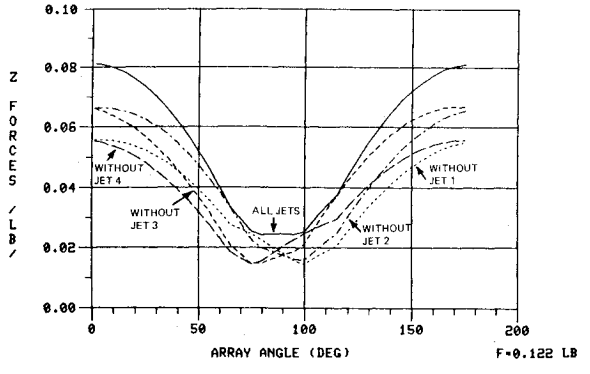

Fig. 12 Design criteria Z plume impingement forces.

Measured vs Predicted Plume Impingement Torques

In order to compare measured vs predicted plume impingement torques, only calibration tests which were performed with all four jets or combinations of calibration tests which, when algebraically summed, provided an effective result from the four jets, were analyzed. These data are listed in Table 2 and plotted in Fig. 13 as a function of solar array angle α. Assuming that the data should be representative of a linear curve over the relatively small range of solar array positions, a least squares polynomial fit was used to generate the dashed lines depicted in Fig. 13. For comparison, the data

Table 2 Satellite plume calibration data[a]

Test no.	$\Delta\phi$, deg	H, in.-lb·s	τ_{xp}, in.-lb	α, deg
	Jets 1 and 2/3 and 4 on array front/back			
1	−0.580	152.42	−0.2688	98.00
17,18	−0.370	157.17	−0.1644	97.04
37	+0.425	148.96	+0.1725	94.94
5	−0.235	151.48	−0.1151	94.10
19,21	+0.330	157.10	+0.1553	94.14
22,24	+0.815	156.95	+0.3767	85.04
	Jets 1 and 2/3 and 4 on array back/front			
(2,3),4	−1.765	157.80	−0.8063	97.01
61	−0.865	148.94	−0.3864	92.04
6,7	−0.825	157.80	−0.3744	91.25
75	+0.155	149.09	+0.0556	87.94
9,10	−0.010	157.80	−0.0002	84.92
11,12	+0.470	157.80	+0.2202	78.59

[a] $\Delta\phi$ = observed satellite roll error change; H = satellite bias momentum level; τ_{xp} = calculated plume torque = $[\tan(\Delta\phi)H/(\Delta t)] - (0.036)F$; F = thrust level = 0.122 lbf; Δt = pulse width = 6.0 s; α = relative solar array position.

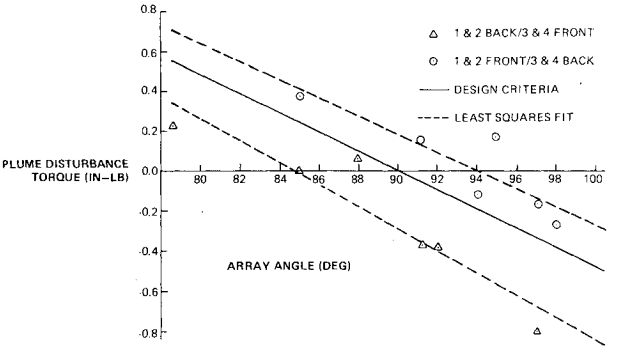

Fig. 13 Satellite flight calibration data vs design criteria plume disturbance torque.

used in designing the satellite attitude control algorithm (the predicted torque multiplied by a factor of two for margin) are also presented in Fig. 13. As can be seen, good agreement exists between the slope of the design criteria data and that of the curves fitted to the flight data. In addition, there seems to be an apparent phase shift with respect to solar array position between the measured and predicted values.

The difference in magnitude (or slope) can be attributed to solar array surface modeling and surface/exhaust gas particle interaction uncertainties, in addition to jet and plume structure modeling uncertainties. The apparent phase shift in solar array position is produced by the different surface properties of the front and back of the solar array (smooth glass solar cells vs honeycomb panels with support ribbing) in addition to solar array deflections due to thermal gradients. This bending occurs when the sun is not normal to the solar array surface, as expected for the design of the thermal insulation associated with the array and support boom.

Conclusions

The nozzle exhaust (far field) plume model for the nominal 0.12 lbf jet as described in this report has been used to analyze and validate the control system used during the north/south stationkeeping maneuver of a three-axis stabilized, momentum-biased satellite similar to that shown in Fig. 1. Three such satellites have been sucessfully launched (12/75, 3/76, and 12/78) and have thus far accomplished all mission requirements satisfactorily. It is thus possible, through the use of this plume model, to predict the expected impingement disturbances acting on a satellite. The stability of a proposed control system influenced by these disturbances can be verified and/or required improvements can be suggested. It is also possible to make a reliable estimate of the fuel required for the designed life of the satellite. It should be emphasized that the plume model described here is appropriate only for the far-field flow regime. It is not intended for studying near-field plume effects which are more complex and more difficult to quantify.

References

[1] Schmidt, G.E., Jr., "The Application of Magnetic Attitude Control to a Momentum Bias Synchronous Communications Satellite," AIAA Paper 75-1055, Aug. 20, 1975.

[2] Keigler, J.E., Lindorfer, W.J., and Muhlfelder, L., "Stabilite Attitude Control for Synchronous Communication Satellites," AIAA Paper 72-572, April 24, 1972.

[3] Cenker, R.J., "Pulsed Modulation of Orbit Adjust Thrusting to Simultaneously Control Roll and Yaw Attitude," AIAA Paper 74-924, Aug. 5, 1974.

[4] Ring, L.R. and Wojciechowski, C.J., "Fairchild ATS-F & G Plume Impingement Study," Lockheed Missiles and Space Co., Huntsville, Ala., Rept. LMSC-HREC D225923, May 1972.

[5] Shapiro, A.H., *The Dynamics and Thermodynamics of Compressible Fluid Flow*, Vol. I, The Ronald Press, New York, 1953.

[6] Emmons, Howard W. (Ed), "Fundamentals of Gas Dynamics," *High Speed Aerodynamics and Jet Propulsion*, Vol. III, Princeton University Press, Princeton, N.J., 1958.